

## Renewable Fuel Utilization in a Cogeneration Arrangement with Hydrate Storage Method\*

Soe NAING\*\*, Takanobu YAMADA\*\* and Kimio NAKANISHI\*\*

\*\*Department of Mechanical Engineering, Kitami Institute of Technology,  
165, Kitami City, Hokkaido 090-8507, Japan  
E-mail: yama@mail.kitami-it.ac.jp

### Abstract

According to the third conference of parties (COP3), Japan has set a target of reducing greenhouse gas emissions by 6% by the year 2010. Many believe that the bulk utilization of fossil fuel influences to the damaging environmental effect. The objective of this paper is to propose an effective method for this goal which is possible to clarify a noticeable utilization of renewable fuel in a micro gas turbine cogeneration system in cold region. Moreover, analysis of renewable fuel, biogas production indicates that production amount becomes largest in hot season, while the total heat energy demand is lowest on during three years. Biogas storage is also adapted for the delay between peak energy supply and demand. Biogas hydrate formation is examined by resource from laboratory experiments and simulation of integration into an existing cogeneration arrangement. The proposed system can be successfully supported the use and reuse of renewable fuel for providing to substantial emission and clean development mechanism for reducing greenhouse gas emission.

**Key words:** Energy Saving, Alternative Energy, Energy Storage, CGS, MGT

### 1. Introduction

Need and use for fuel and energy are both particular roles throughout mankind history and is simultaneously related the environmental issues such as air and water pollutions, and global climate change. Indigenous fuel and energy resources for industrialized nations are extremely begun to come to the fore. In this paper, the potential performance benefits of adding a fuel storage process to a cogeneration system (CGS) are examined. Biogas is one of the most attractive fuels because it involves methane close to 60 v-%, which can be renewably produced with fermentation process of sewage. It is also an under-utilized energy resource than can be expected to be particularly useful in cold regions and yet the total performance of this approach in practice remains to clarify adequately. In this investigation, the CGS at Kitami City Sewage Treatment Center in Japan is adopted for simulations and experiments, and formation of methane hydrate (MH) is also tried to perform biogas hydrate storage. Electrical power and heat energy are produced by a series of micro gas turbines (MGTs) driven by the combustion of biogas captured from the sludge fermentation process<sup>(1)</sup>. The temperature of air at the compressor inlet stage of the MGT is employed as an important parameter to determine its performances. The energy in-out method and effectiveness-*NTU* relationship are used in simulation procedure of the CGS<sup>(2)</sup>. As the rate of biogas production by an anaerobic fermentation digester varies over the course of a year, typically in an opposite trend to the variation in the seasonal power and energy demand, a method for storing biogas is expected to be beneficial<sup>(3)</sup>. Methane hydrate has been investigated by a number of researchers as a cool energy storage method with useful storage and recovery properties<sup>(4)</sup>. Storage at higher temperature by utilizing the ice barrier formed by dissociated hydrates may also provide advantages for reuse and fuel storage.

## Nomenclature

- $A_i$  : transversal surface area,  $m^2$   
 $C_p$  : specific heat of water,  $J/g\ K$   
 $Fl$  : flow rate of compressor for biogas hydrate,  $m^3/h$   
 $G_{ice}$  : ice mass occupied quantity,  $g$   
 $h(t)$  : enthalpy,  $kJ/kg$   
 $M_m$  : molecular weight of methane,  $g/mol$   
 $m_{fuel}$  : fuel consumption,  $m^3/h$   
 $m_{mgt}$  : mass flow rate at exhaust stage of MGT,  $kg/s$   
 $m_{slu}$  : sludge amount in digester,  $kg/s$   
 $m_w$  : mass flow rate of heat exchanger cold side,  $kg/s$   
 $M_w$  : molecular weight of water,  $g/mol$   
 $n_r$  : rotating speed of MGT,  $rpm$   
 $P_{ele}$  : electrical power demand of each machine,  $kW$   
 $P_f$  : final pressure of hydrate system,  $MPa$   
 $P_i$  : initial pressure of hydrate system,  $MPa$   
 $P_u$  : required power for stable formation of hydrate,  $kW$   
 $Q_{th, ehr}$  : heat recovery,  $kW$   
 $Q_{th, exe}$  : exhaust heat from MGT,  $kW$   
 $Q_{th, fuel}$  : fuel thermal energy,  $kW$   
 $Q_{th, loss}$  : losses heat from MGT,  $kW$   
 $Q_l$  : heat loss from digester,  $kW$   
 $Q_n$  : necessary heat demand for sludge treatment,  $kW$   
 $R_m$  : gas constant of methane,  $J/kg\ K$   
 $t_d$  : necessary temperature for sludge treatment,  $^{\circ}C$   
 $t_{exe}$  : exhaust temperature of MGT,  $^{\circ}C$   
 $T_f$  : final temperature of methane hydrate,  $^{\circ}C$   
 $T_i$  : initial temperature of methane hydrate,  $^{\circ}C$   
 $t_{iEXE}, t_{oEXE}$  : inlet and outlet temperatures of heat exchanger cold side,  $^{\circ}C$   
 $t_N, t_{amb}$  : normal and ambient temperature,  $^{\circ}C$   
 $t_{out}$  : outlet temperature of heat exchanger hot side,  $^{\circ}C$   
 $t_u$  : temperature of inflow sludge,  $^{\circ}C$   
 $V_e$  : methane hydrate volume,  $m^3$   
 $\alpha_1, \alpha_2$  : heat transfer coefficient,  $W/m^2\ K$   
 $\delta_i$  : thickness in the direction of heat flow,  $m$   
 $\lambda_i$  : thermal conductivity,  $W/m\ K$

## 2. Overview of the system

Plenty produced amount of renewable fuel, biogas from anaerobic digester is considered both as a combustion fuel for prime mover in a CGS and for storage by hydrate formation. Figure 1 shows schematic layout of the CGS with renewable fuel utilization. It is mainly composed of renewable fuel production system, the CGS and hydrate storage system. The corresponding standard specifications for each system are listed in Table 1.

In order to obtain renewable fuel from sewage waste, anaerobic fermentative system is generally installed in sewage treatment feasibilities. The electrical power and heat energy demand are investigated on results of the existing renewable fuel production process. Electricity is supplied to its demand by operating the MGT generator and by purchasing electricity from an electrical power company. Exhaust heat generated from the MGT is recovered by heat recovery system to produce heat supply for its demand. Ambient air enters a generator and passes systematically through a centrifugal compressor, a

recuperator, an annular combustion chamber, and a radial turbine. The rotating components of the MGT are mounted on a single shaft supported by air bearings. The generator is cooled by the inlet air, and simultaneously produces both electrical power and exhaust heat energy. The exhaust heat transforms to heat recovery by using a heat exchanger and it is assumed as a shell and tube heat exchanger with effectiveness of 75%. The increase in performance of a CGS by implementation of an MH storage system is examined using data from (1) renewable fuel production system, (2) the CGS and (3) biogas hydrate system assuming that it is equipped at the sewage treatment center.

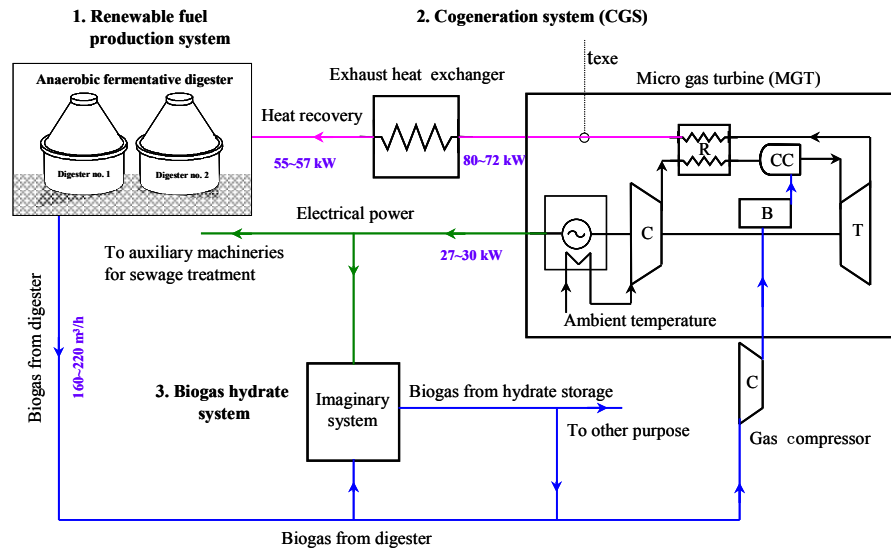


Fig. 1 Configuration of a CGS with renewable fuel and hydrate storage

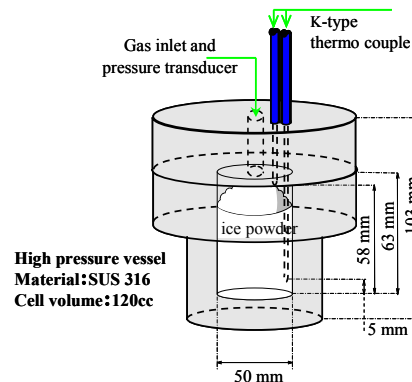


Fig. 2 Schematic of high pressure vessel for MH formation

Table 1 Standard specification of equipments

<b>Renewable fuel production process</b>		Flow rate of vacuum pump	12 ~ 15 L/min
Size of digester	H: 24m, D: 16m	Speed of vacuum pump	1250 ~ 1500 rpm
Flow rate of biogas production	160 ~ 220 m <sup>3</sup> /h	Maximum allowable pressure	10 MPa
Fuel consumption	17 ~ 20 m <sup>3</sup> /h	Volume occupancy of low temperature freezer	465 L
<b>CGS</b>		Maximum allowable temperature	-40 ~ + 100 °C
Rated speed of MGT	96,000 rpm	<b>Biogas hydrate simulation (imaginary system)</b>	
Rated output power of MGT	30 ± 2 kW	Electricity demand for vertical gas compressor	11 kW
Rated electrical efficiency of MGT	26 ± 2 %	Electricity demand for block ice slicer	3 kW
NO <sub>x</sub> emission from MGT	< 9 ppmV@ 15%O <sub>2</sub>	Electricity demand for low temperature freezer	2.5 kW
Exhaust heat exchanger	shell & tube exchanger	Flow rate of vertical gas compressor	34 m <sup>3</sup> /h
Effectiveness of heat exchanger	75 %	Capacity of block ice slicer	2.2 kg/min
<b>MH formation</b>		Number of vertical gas compressors	1
Material of high pressure vessel	SUS 316	Number of block ice slicers	2
Cell volume	120 mL	Number of low temperature chambers	4
Cell size (inner diameter × height)	φ50 × 63 mm		

Since biogas hydrate shows the similar formation as the case of MH, the possibility of gas storage is investigated by attempting the MH formation using a 120mL high-pressure vessel made of stainless steel to estimate its formation ratio. Figure 2 shows the schematic of high pressure vessel for MH formation. In this experiment, the vessel is filled with methane and ice powder prepared using a block ice slicer. It is assumed in actual case that block ice will be made from frozen process water of sewage treatment. The vessel is soaked in a low-temperature freezer, and the pressure and temperature of the MH are measured throughout the experiment. In the investigation, it is assumed that actual MH formation speed is just same as in experiment and this biogas hydrate system is considered as imaginary system. Other components for this imaginary system are composed of four 2.5kW low-temperature freezers, two 3kW block ice slicers, and an 11kW vertical gas compressor.

### 3. Heat demand for renewable fuel production

Anaerobic treatment for complex wastes involves two distinct stages which are the acid fermentation stage and the methane fermentation stage. The end products of the acid fermentation stage are converted to gases by several different species of anaerobic bacteria. The bacteria responsible for acid fermentation and for methane fermentation are relatively tolerant to changes in temperature. According to The Environmental Engineering Handbook, Lawrence proposes that temperature range required for activated sludge treatment in the anaerobic digestion process is typically 20 to 35°C <sup>(5)</sup>. However, the Kitami's digester operates at necessary temperature of 39°C due to the cold location and the characteristics of the operating system. Steam is employed as the heating source for the heating process and for activating sludge treatment.

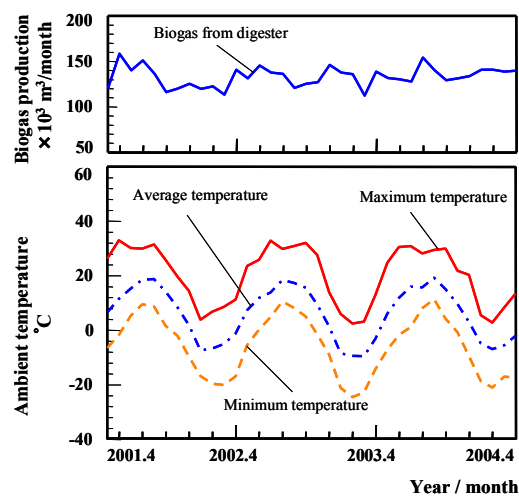


Fig. 3 Influence of seasonal change to biogas production in Kitami City

Figure 3 shows biogas production rate and ambient temperature of seasonal change in Kitami City. Ambient temperatures are obviously fluctuated and also influence to renewable fuel, biogas production rate. Maximum and minimum temperature in average temperature range is around 20°C and -6°C, respectively. To avoid the confusion of the procedure, it can be divided into hot season and cold season with respect to ambient temperature. After digesting in anaerobic fermentative process, biogas is variously produced with seasonal variation of sludge quantities and ambient temperatures. It may be investigated from actual process that the rate of biogas production varies hourly within the range of 160 to 220m<sup>3</sup>/h. It is obviously shown in figure that the production rate in hot season is larger than the rate in cold season.

If heat gain from current solar radiation energy on the digester is negligible, total heat

energy demand is combination of heat loss from digester, air conditioning demand for buildings and necessary heat demand for sludge treatment. Heat loss from digester to surroundings greatly affects the digester's total heat energy demand and loss energy is higher in cold season than in hot season. If ( $K_i$ ) denotes heat transfer coefficient at  $n$  number of material layers in digester wall, heat loss from digester to surroundings ( $Q_l$ ) can be estimated:

$$Q_l = K_i \times A_i (\Delta T) \tag{1}$$

$$\frac{1}{K_i} = \frac{1}{\alpha_1} + \sum_{i=1}^n \left[ \frac{\delta_i}{\lambda_i} \right] + \frac{1}{\alpha_2} \tag{2}$$

Temperature difference ( $\Delta T$ ) directly depends on inner and outer surface temperatures which may be noted as necessary temperature for sludge treatment and average ambient temperature. Heat transfer coefficients ( $\alpha_1, \alpha_2$ ), thickness in the direction of heat flow ( $\delta_i$ ) and thermal conductivity ( $\lambda_i$ ) can be obtained from catalog data of digester with regard to constructing material and structure. Air conditioning demand is calculated based on two small buildings equipped with control units and machines. Average ambient temperature is also calculated in this air conditioning procedure. If sludge amount in digester ( $m_{slu}$ ) is known in working process, according to the definition of heat capacity, necessary heat demand for sludge treatment ( $Q_n$ ) is defined as:

$$Q_n = m_{slu} \times C_p (t_d - t_u) \tag{3}$$

If necessary temperature for sludge treatment ( $t_d$ ) is equal to 39°C, temperature of inflow sludge ( $t_u$ ) is assumed as a range of 10 to 12°C with respect to inlet pre-heating system of sewage treatment plant. Specific heat of waste water ( $C_p$ ) varies slightly with temperature and the specific heat of natural water, a value of 4.19 J/g K could be used. It can be noted that necessary heat demand can vary on sludge quantity and temperature of inflow sludge.

Figure 4 shows the electrical power and heat demand for renewable fuel production in the past three years. Electrical power and heat demand are investigated based on actual demand of present renewable fuel production process. Digester heat losses and air conditioning demand are fluctuated with respect to ambient temperatures. The necessary heat demand also varies in characteristic curve. To consider the total heat demand, it is obviously grown up to reach its maximum demand in cold season. As mention to Fig. 3 and 4, it is clearly noted that the maximized mass productions of biogas are produced in hot season, while the system may demand the minimized heat energy.

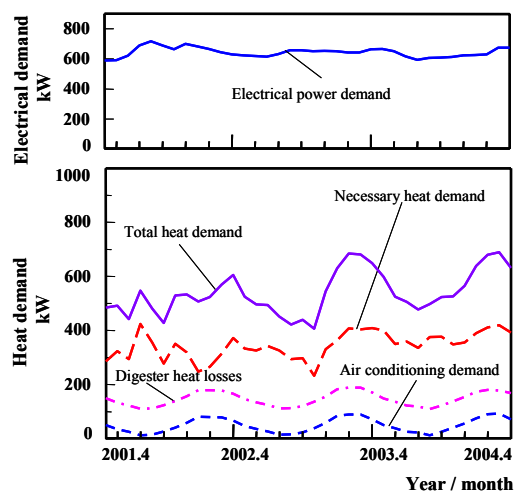


Fig. 4 The electrical power and heat demand

#### 4. Fuel utilization in a CGS

Figure 5 shows simplified schematic of the topping-cycle of the CGS while the system consumes renewable fuel, and produces electrical power and heat energy. The performance characteristics of the CGS are determined by ambient temperature as a particular parameter that results in a large temperature difference between hot and cold season.

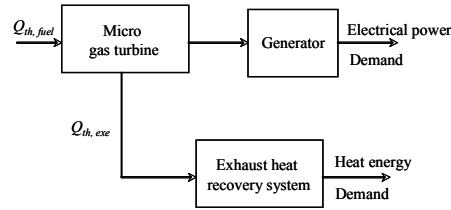


Fig. 5 Simplified diagram of a CGS

Obviously, several researchers have proposed that cooling effect on compressor inlet air can increase the cycle efficiency and reduce the exhaust temperature of MGT<sup>(6)-(8)</sup>. It is found that electricity generation efficiency is remarkably increased when the experiments are operated in low ambient temperature condition. In this operation characteristic of MGT, the temperature difference between the ambient stage and the compressor inlet stage reaches typically 10 to 12°C. Brayton open-cycle analysis (neglecting the gas composition in exhaust flue gas) gives temperatures, specific heat capacities at constant pressure and other necessary parameters of a MGT to be calculated. The effectiveness of recuperator in MGT is found to be 68% assuming a combustion chamber outlet temperature of 850°C. If exhaust gas temperature is distributed in a range of 200 to 400°C, the enthalpy of exhaust gas ( $h$ ) value may be evaluated as:

$$h(t) = \left[ 65.275 + 239.566 \left( \frac{t}{1000} \right) + 2.923 \left( \frac{t}{1000} \right)^2 + 36.76 \left( \frac{t}{1000} \right)^3 - 16.70 \left( \frac{t}{1000} \right)^4 \right] \times 4.19 \quad (4)$$

If ambient temperature ( $t_{amb}$ ) is normally changed under atmospheric conditions, corrected rotating speed ( $n_{cor}$ ) is:

$$n_{cor} = \sqrt{\frac{t_N}{t_{amb}}} \times n_r \quad (5)$$

Corrected rotating speed greatly affects to mass flow rate of the MGT ( $m_{coa}$ ), which may be expressed as follows:

$$m_{coa} = (4.2227 \times 10^{-11} n_{cor}^2) - (2.5051 \times 10^{-7} n_{cor}) + 0.025 \quad (6)$$

$$Q_{th,fuel} = m_{fuel} \times LHV_{biogas} \quad (7)$$

Input thermal energy of the fuel in MGT ( $Q_{th,fuel}$ ) may be calculated and it is based on lower heating value ( $LHV_{biogas}$ ) and biogas fuel consumption ( $m_{fuel}$ ), 21.5MJ/m<sup>3</sup>, 17-20m<sup>3</sup>/h for 27-30kW of power, respectively. The exhaust energy may be recovered by using the exhaust enthalpy, the exhaust gas mass flow rate and the thermal utility levels of recovery devices in a shell and tube heat exchanger. Necessary parameters and performances of working fluid, water are simulated in the heat medium of anaerobic digester by using the effectiveness-NTU relationship. The amount of heat losses may be calculated from the outlet temperature of heat exchanger and ambient temperature. If exhaust gas mass flow rate ( $m_{mgt}$ ) is linked to the MGT mass flow rate, exhaust heat energy ( $Q_{th,exe}$ ), exhaust heat loss ( $Q_{th,loss}$ ), and exhaust heat recovery ( $Q_{th,ehr}$ ) may be defined as:

$$Q_{th,exe} = m_{mgt} [h(t_{exe}) - h(t_{amb})] \quad (8)$$

$$Q_{th,loss} = m_{mgt} [h(t_{out}) - h(t_{amb})] \quad (9)$$

$$Q_{th,ehr} = m_w [h(t_{iEHE}) - h(t_{oEHE})] \quad (10)$$

Overall thermal efficiency with or without storage are defined as a ratio of total heat recovery and total electrical power to *LHV* of methane in biogas.

Figure 6 (a) shows the influence of ambient temperature on mass flow rate and exhaust temperature of the MGT. Although the exhaust temperature is increased with the increase of ambient temperature, the mass flow rate and it results in the decrease of MGT speed. The standard air mass flow rate in manufacturer supported data is equal to 0.31kg/s that may be 0.061kg/s lower than the simulated value at an ambient temperature of 15°C. The range of simulated exhaust temperature shows 245 to 298°C, and the range of simulated mass flow rates show 0.41 to 0.35kg/s. With regard to exhaust heat energy definition, exhaust heat amount decreases due to the reduction of  $m_{mgt}$ , although the exhaust temperature is increasing. Since, high ambient temperature makes the air density low, and resultant of low mass flow rate into the MGT reduces exhaust heat energy. Figure 6 (b) shows the enthalpy of compressor inlet and exhaust stage. It can be noted that slope of those two enthalpies must show nearly the same increasing tendency in operation and those are also agreed with the experimental data.

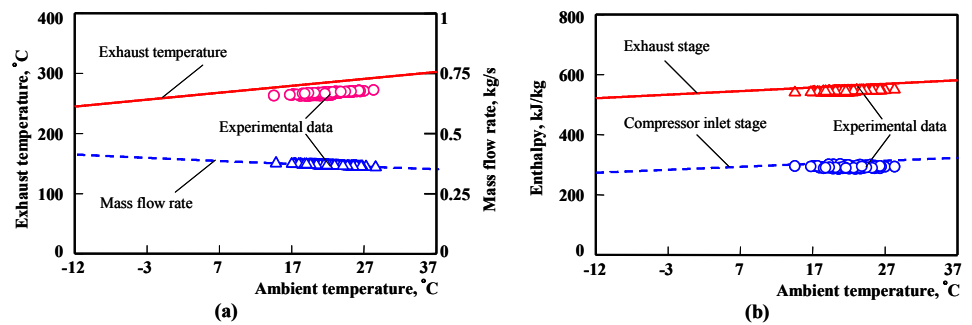


Fig. 6 Some parameter of the MGT

Figure 7 (a) shows produced heat and power from MGT. Figure 7 (b) also shows the heat to power ratio, exhaust heat recovery and losses on ambient temperature. When the ambient temperature exists in the range of 17 to 27°C, the exhaust heat produces acceptable values from 80 to 72kW and exhaust heat recovery is in the range of 55 to 57kW. Electrical power can be found in the range of 28 to 22kW to ambient temperatures. Several researchers have proposed optimization schemes for exhaust heat energy and heat recovery from the viewpoint of energy supply and demands included its cooling or heating demand<sup>(9)</sup>,<sup>(10)</sup>. In this paper, exhaust heat and exhaust heat recovery is optimized to meet the total heat demand of renewable fuel production process.

In the Fig. 7 (b), the simulated exhaust heat to power ratio is gradually decreasing with the increase of ambient temperature and then it is increasing over 24°C again. Heat to power ratios vary in the range of 2.6 to 3.2 and are in good agreement with the experimental data.

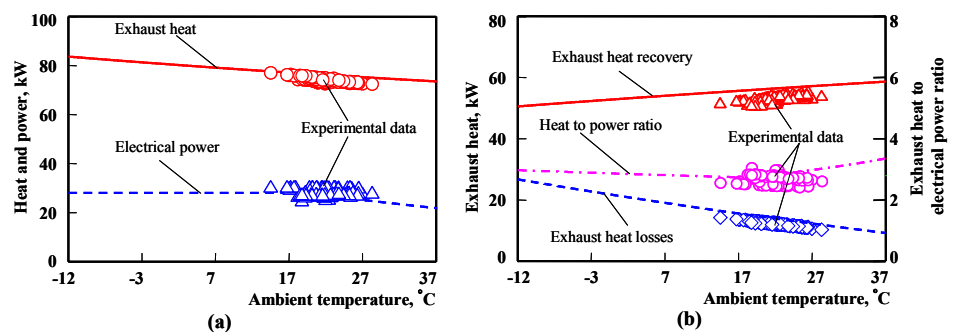


Fig. 7 Performance of the MGT

It may be caused as different slope between exhaust heat and power. It shows that the drop of the electrical power output is larger than drop of simulated exhaust heat in an ambient temperature range of 20 to 37°C. This fact suggests that electrical power is more sufficient in low ambient temperature up to 20°C. At the optimal ambient temperature range, good electrical power may be obtained with acceptable levels of exhaust heat recovery.

Although the simulated exhaust heat recovery is slightly higher than the corresponding experimental values, those results demonstrate that heat recovery can be increased significantly and the exhaust heat loss can be reduced at the high ambient temperatures. To apply the necessary heat demand for digester sludge treatment process, an optimized ambient temperature is estimated as 20°C. It may be shown that the maximum exhaust heat recovery of 57kW is attained, which corresponds to a net electrical power output of 27.8kW. As mentioned and known, heat recovery ability of the simulated cogeneration plant possesses 74% of the total MGT exhaust heat. It is nearly equal to 5% greater than heat recovery ability of the existing cogeneration plant which is operated with different heat exchanger in the heat recovery system. Considering an optimized approaching method, resultants of the simulated cogeneration system will be applied in multiple MGTs simulation for renewable fuel production process, except the piping losses. Table 2 shows electrical power output and heat simulated from multiple numbers of MGTs operation. It is found that exhaust heat recovery is equal to 513kW when electrical power is 250kW at ambient temperature of 20°C.

Table 2 Resultants in multiple MGTs simulation

Number of MGTs	Exhaust heat output (kW)	Exhaust heat recovery (kW)	Electrical power output (kW)
1	76	57	27.8
9	684	513	250.2

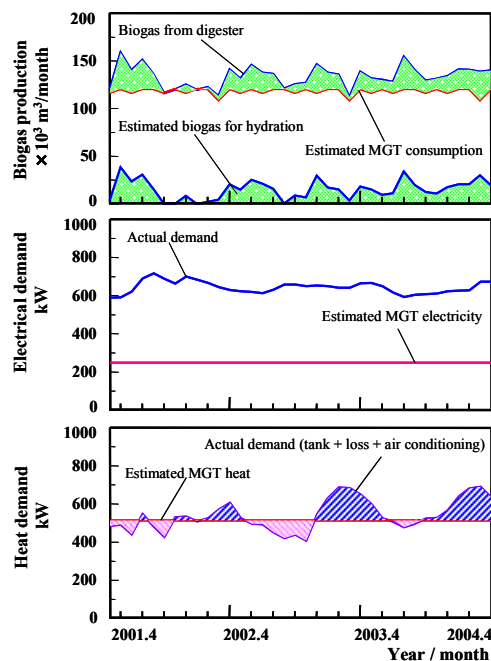


Fig. 8 Estimated electrical power and heat from MGTs

Figure 8 shows the influence of estimated heat and electrical power from the MGTs on actual production and demands of Kitami Sewage Treatment Center to the past months. Nine MGTs produce the sufficient amount of exhaust heat recovery and acceptable



electrical power for renewable fuel production process. According to biogas production result, consumption amount of nine MGTs is enough to produce biogas. Estimated biogas for hydrate storage is expressed in the shaded area that is nearly 12% of the total biogas production. The electrical power demand of Kitami Sewage Treatment Center is always substantially higher than the estimated electrical output of the MGTs. Moreover, actual heat demand in shaded forms is obviously obtained with under and over of estimated MGTs supplied heat. As mentioned and known, actual heat demand must face its maximum demand in cold season, because the biogas production rate is higher in hot season than in cold season. To solve the imbalance, various methods for gas storage have been proposed to store some proportion of evolved biogas effectively. In this paper, biogas hydrate storage method is proposed by using practical integration of the MH.

### 5. Practical integration of MH

MH formation is an effective fuel storage method that also supports the clean development initiative. The absolute hydration mass ( $G_{mab}$ ) in Eq. (11) is given by the difference between the initial methane mass and the rejection methane mass, which involves the methane hydrate volume and the gas constant of methane. The methane occupied mass ( $G_m$ ) in Eq. (12) is calculated from the molecular weight ratio of water to methane and the occupied mass of ice. The MH formation ratio ( $\eta_h$ ) is defined as the ratio of absolute hydration mass to methane mass occupied in the ideal guest/water ratio for molecules, and is finally expressed as:

$$G_{mab} = \left[ \frac{(P_i + 0.08) \times 10^9 V_e}{(273.15 + T_i) R_m} \right] - \left[ \frac{(P_f + 0.08) \times 10^9 V_e}{(273.15 + T_f) R_m} \right] \quad (11)$$

$$G_m = \frac{8}{46} \times \frac{M_m}{M_w} \times G_{ice} \quad (12)$$

$$\eta_h = \frac{G_{mab}}{G_m} \times 100 \quad (13)$$

Figure 9 (a) shows the equilibrium pressure, hydration temperature of MH in the laboratory experiment. The initial pressure range of 4 to 7MPa is successfully examined. It is clearly shown that lower pressure, the case for 4MPa can early give stable equilibrium condition, even though its hydrate formation ability is smaller than in the case of higher pressures. However, if the system is used under high pressure conditions, the hydrate formation temperature will not need to be lowered. At the case for 7MPa, temperature is increased to reach maximum temperature or 4°C in 20 hours after starting experiment. Figure 9 (b) shows formation ratio in hydrate mole consumption of MH. It may be observed that MH hydrate formation ratio is usually sensitive to both of temperature and pressure. In this experiment, the system temperature is held in the range of -1 to 1°C. To consider MH formation ratios due to four initial pressure cases, the ratio in the case of 4MPa shows one-third of the ratio in the case of 7MPa. In order to obtain the optimal benefit, the MH ratio of 70% in the case of 7MPa is chosen and the subsequent biogas simulation is executed.

Bulk biogas is produced by a solid waste digester typically includes methane (50-60%), carbon dioxide (38-48%) and trace components (2%). In the simulation, biogas is assumed to consist of 60% methane and 40% carbon dioxide. Figure 10 shows comparison of the 100% methane and the biogas mixture (60% methane, 40% carbon dioxide) by using the CSMHYD program<sup>(4)</sup>. The simulated equilibrium pressure for methane is 3-5% greater than those obtained in the laboratory experiment at a system temperature of 273±1K. The simulated equilibrium pressure for the biogas mixture is lower than the pressure for methane, indicating that carbon dioxide depresses the equilibrium pressure at a given temperature. The reported lower and upper quadruple points of carbon dioxide hydrate are

273.1K and 283.0K <sup>(4)</sup>, while the quadruple point of methane is 272.9K. Carbon dioxide hydrate has been suggested that it has higher thermodynamic stability than with methane hydrate. In this study, it should be noted that biogas formation ratio is assumed to equal MH ratio of 7MPa case when the influence of carbon dioxide in hydrate formation is ignored.

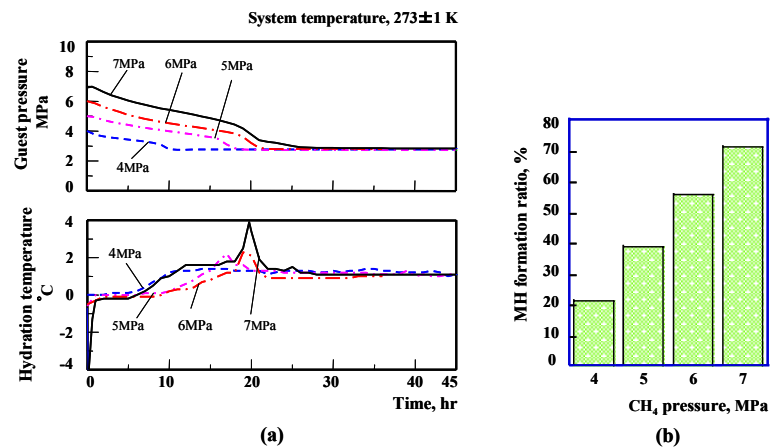


Fig. 9 Experimental results for the MH formation

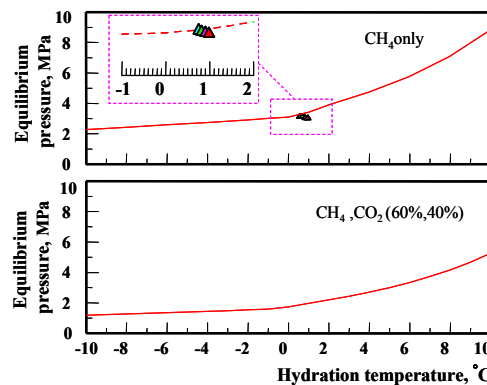


Fig. 10 Pressure prediction at given temperature by using CSMHYD programming

A small high-pressure cylinder which is used in the experiment for the formation of biogas hydrate, and the formation ratio of the MH is measured. Necessary specifications of the required machineries for biogas hydrate are listed in Table 1. Required power for stable hydrate storage is simulated, based on biogas flow rate of compressor, electrical power consumptions of each machine and biogas formation ratio. If electrical power demand ( $P_{ele}$ ) of each machine and flow rate ( $Fl$ ) can be obtained from catalog data, required power for stable hydrate storage ( $P_u$ ) can be defined as:

$$P_u = \sum_{i=1}^n \frac{P_{ele_i}}{Fl \times \eta_h} \quad (14)$$

In this simulation, flow rate ( $Fl$ ) is assumed as standard flow rate of the vertical gas compressor which is dependent on desired biogas capacity. Since MH formation speed and ratio strongly depend on storage pressure and temperature, actual size and shape of storage vessel are not specified for flow rate of 34m<sup>3</sup>/h yet. Number of machineries ( $n$ ) represents the quantity of collected necessary machineries for the simulation. At hydration temperatures of 268 to 273K and their pressures of 1 to 5MPa condition, the required power for stable hydrate storage is predicted to be a value of 1.13kWh/m<sup>3</sup> for biogas.

To observe the CGS with hydrate storage method, the summarized results are shown in Fig. 11 and Fig. 12. The actual power demand, the estimated electricity of MGTs and

estimated electrical demand for hydration are obviously investigated. The estimated electrical demand rate for hydrate storage is 16MWh/month and it is only 9% of the estimated electricity of MGTs which is related to 39% of total actual power demand for the whole process. The estimated reuse energy rate from storage device is 33MWh/month in process with storage devices. Reuse energy rate from biogas hydrate is only 36% of the estimated total energy from storage device. It should be noted that the estimated total energy from biogas hydrate storage can successfully recover the necessary energy in CGS.

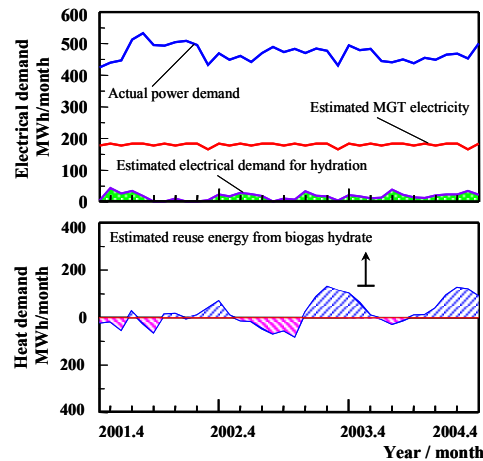


Fig. 11 Results for integration of biogas storage

According to biogas production process, surplus biogas in process without storage devices is released and usually burned with auxiliary boilers. Since they realize nearly same characteristics to combustion process of MGT, the amount of CO<sub>2</sub> emission without storage devices are almost same as the emission with storage devices. As mention to Fig. 12, total estimated MGTs consumption is  $4257 \times 10^3 \text{ m}^3$  that is nearly 88% of total biogas production. It should be expected that small amount of evolved total biogas is needed to make up biogas hydrate storage. Estimated excess energy rate from biogas hydrate storage is 57MWh/month and it may be 64% of the estimated total energy rate from biogas hydrate. Those estimated excess energy may be used for other purposes. This simulation demonstrates that biogas hydrate storage is an effective method for balancing the fluctuating biogas production rate and energy demand through a year. It may prevent the release of excess biogas produced in the hot season and secure an energy source for use in periods of high energy demand in the cold season. Overall thermal efficiencies with and without storage devices reach to 70% and 64% of total energy from biogas, respectively. It may be noted that the proposed system may effectively support to reuse biogas remained in process. This proposal also supports the clean development initiative and reduces greenhouse gas emissions.

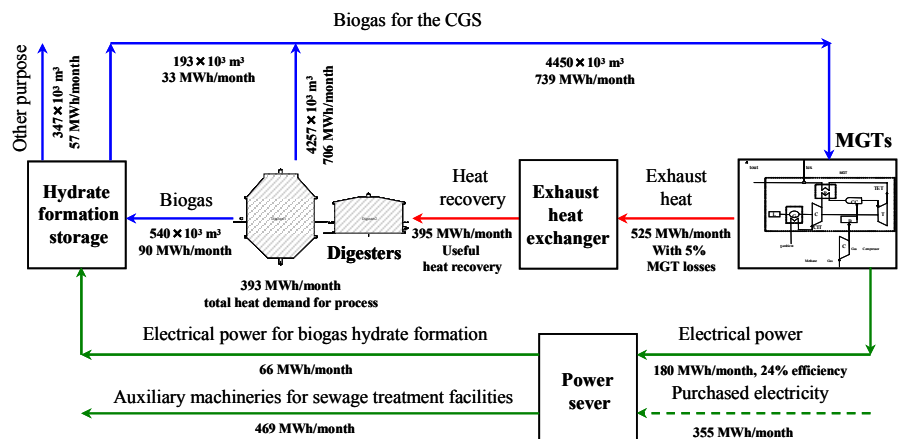


Fig. 12 Schematic for summarized results with storage device

## 6. Conclusion

In this paper, renewable fuel production and utilization has been successfully investigated by examining the related optimal number of the MGTs in cogeneration arrangement and the maximum electrical power and heat energy demand under various conditions based on existing Sewage Treatment Facilities. Moreover, a proposed balanced method with biogas hydrate storage has been carried out in the past three years.

Various ambient temperatures greatly influence biogas production process and the performance of CGS. Biogas plant is usually constructed in large capacity which is to treat the maximum input sludge quantities and the process necessities. The mass flow rate of the MGT also obviously influences the thermal energy of the CGS. The performance of the CGS plant can be increased by installing the inlet temperature cooling system in its process.

The total electrical power demand of an anaerobic fermentation process has been demonstrated to be substantially higher in cold regions, while acceptable heat energy can be obtained within the ambient temperature range of 17 to 27°C. The renewable fuel has been effectively utilized in approaching methods of direct consumption and reused consumption by the multiple numbers of MGTs. Biogas hydrate storage has been successfully supported to imbalance cause between renewable fuel production and its demands. The proposed system has supported the recovery of energy from waste, providing a clean development mechanism for reducing greenhouse gas emissions.

## References

- (1) Yamada, T., Yamada, T., and Nakanishi, K., Applied research for a Sewage Treatment Center at cold region with MGT cogeneration system, *Proceedings of Symposium on Environmental Engineering of JSME*, No. 05-13, Japan, 2005, pp. 462-465.
- (2) Naing, S., Yamada, T., Yoshinaga, N., and Nakanishi, K., Cycle Analysis of Cogeneration System with Biogas and its Hydrate Formation, *Proceedings of the 2<sup>nd</sup> International Workshop and other Related Topics*, Kitami, Japan, 2005, pp. 87-93.
- (3) Naing, S., Yamada, T., and Nakanishi, K., "Analysis of micro gas turbine cogeneration system with biogas storage," *Proceedings of 4<sup>th</sup> International Energy Conversion Engineering Conference and Exhibit (IECEC)*, AIAA 2006-4183.
- (4) Sloan, E. D., jr., *Clathrate hydrates of natural gases*, 2<sup>nd</sup> ed., Marcel Pekker, New York, 1997, Chaps. 1.
- (5) Davis, M. L., and Cornwell, D. A., *Environmental Engineering Hand Book*, 3rd ed., the McGraw-Hill Companies, Inc. Singapore, 1998.
- (6) Yokoyama, R., and Ito, K., "Effect of Inlet Air Cooling by ice storage on Unit Sizing of a Gas Turbine Cogeneration Plant," *ASME Journal*, Vol. 126, Apr. 2004, pp. 351-357.
- (7) Bhargava, R., Bianchi, M., Melino, F., and Peretto, A., "Parametric Analysis of Combined Cycles Equipped with Inlet Fogging," *ASME Journal*, Vol. 128, April, 2006, pp.326, 334.
- (8) Chmielniak, T., Kosman, G., and Kosman, W., "Analysis of cycle configurations for the Modernization of Combined Heat and Power Plant by Fitting a Gas Turbine System," *ASME Journal*, Vol. 126, Oct. 2004, pp. 816-822.
- (9) Sancho-Bastos, F., and Perez-Blanco, H., "Cogeneration system simulation and control to meet simultaneous power, heating and cooling demands," *ASME Journal of Engineering for Gas Turbines and Power*, Vol.127, 2005, pp. 405-409.
- (10) Gamou, S., Yokoyama, R. and Ito, K., "Parametric study on Economic Feasibility of Micro turbine Cogeneration Systems by an optimization approach", *ASME Journal of Engineering for Gas Turbines and Power*, Vol. 127, 2005, pp. 389-396.